

# Efficient Nonlinear Distortion Analysis of RF Circuits

Dani Tannir and Roni Khazaka  
Department of Electrical and Computer Engineering  
McGill University  
Montreal, Canada, H3A 2A7  
dani.tannir@mail.mcgill.ca, roni.khazaka@mcgill.ca

## Abstract

*Nonlinear distortion, typically defined using the third order intercept point (IP3), is one of the key figures of merit that are critical in the design of RF communication circuits. The calculation of IP3 is typically based on analytical approaches such as Volterra Series which are very complex and difficult to apply to circuits of arbitrary complexity, or on simulation based methods which require multi-tone inputs and thus result in a very high CPU cost. In this paper a new method based on the computation of the circuit moments is proposed. The new approach uses the circuit moments in order to numerically compute the Volterra kernels. This automates the process of numerically obtaining such kernels for any circuit and results in an efficient approach for the computation of IP3.*

## 1. Introduction

Radio Frequency (RF) communication circuits such as Low Noise Amplifiers (LNAs) and mixers have become a staple in modern electronics and products. This has put a significant emphasis on efficient design and a reduced time to market for much applications which can only be achieved using more effective simulation and design automation tools. However such simulations, which require obtaining the steady-state solution of a nonlinear circuit due to a sinusoidal input, present a significant challenge using conventional spice-like simulators because a very large number of cycles is required before the steady-state solution is reached. The Harmonic Balance method [4], [5], [7], addresses this problem but results in a large system of nonlinear equations with a dense Jacobian. In this paper, we do not address the general problem of nonlinear steady-state simulation, but we rather focus on one of the key design requirements for RF circuits which is linearity [8]. Linearity affects the intermodulation distortion and is commonly characterized by the third order intercept point (IP3) [11].

The computation of IP3 is one of the most CPU intensive parts of RF circuit simulation due to the large number of tones present [10].

There are two classes of techniques for computing the IP3 of a circuit. The first is based on analytical approaches such as the Volterra functional series [6]. Such methods require complex analytical manipulations and are difficult to automate for arbitrary circuit topologies [1], [9]. The other class of methods relies on brute force simulation and mimics laboratory measurements by simulating the circuit using two input tones and noting the solution that corresponds to the intermodulation product at  $2\omega_1 - \omega_2$ . The main disadvantage of this approach is that the multi-tone inputs result in a significantly higher number of harmonics and thus a large number of nonlinear equations in the Harmonic Balance (HB) simulation. This in turn results in a high CPU cost.

In this paper a method based on the computation of the circuit moments is proposed for obtaining IP3. The new approach can be shown to be equivalent to computing the values of the appropriate Volterra kernels at the frequencies of interest. This approach does not require any analytical manipulation but is rather applied directly to the MNA [3] formulation of the circuit. It can therefore be applied to circuits of arbitrary complexity. Furthermore, the computation of all the moments only requires one LU decomposition of the Jacobian evaluated at the DC point which is very sparse unlike the typical Harmonic Balance Jacobian which is usually both large and dense, especially for large RF circuits that exhibit strong nonlinearities. Finally, the computation is done numerically with the input frequencies known, and thus produces very accurate results.

This paper is organized into six sections. Following the introduction, Section 2 outlines the formulation of a system and Section 3 highlights the brute force approach for obtaining IP3. The proposed method is then presented in Section 4. Numerical examples are shown in Section 5 in order to illustrate the accuracy of the new method, followed by conclusions in Section 6.

## 2. MNA system formulation

Consider a non-linear circuit excited by one or more input tones. The Modified Nodal Analysis (MNA) [3] circuit equations can be expressed in the time domain as

$$\mathbf{G}\mathbf{x}(t) + \mathbf{C}\dot{\mathbf{x}}(t) + \mathbf{f}(\mathbf{x}) = \mathbf{b}(t), \quad (1)$$

where  $\mathbf{x}(t) \in \mathbb{R}^n$  is the vector of  $n$  unknown node voltages, inductor and voltage source currents, nonlinear capacitor charges, and nonlinear inductor fluxes.  $\mathbf{G} \in \mathbb{R}^{n \times n}$  contains the circuit stamps of the linear memoryless elements,  $\mathbf{C} \in \mathbb{R}^{n \times n}$  contains the memory elements,  $\mathbf{f}(\mathbf{x}) \in \mathbb{R}^n$  is a vector of nonlinear functions, and  $\mathbf{b}(t) \in \mathbb{R}^n$  contains the independent input sources.

## 3. Simulation based brute force approach

The third order intercept point can be found by solving for the steady-state solution due to a two-tone input (for example  $\omega_1$  and  $\omega_2$ ) and considering the intermodulation term at  $2\omega_2 - \omega_1$ . This can be achieved using the Harmonic Balance approach by expressing the periodic solution as a truncated series of sine and cosine functions at the harmonics of the inputs as well as at the intermodulation products. This results in a set of nonlinear algebraic equations in the form

$$\bar{\mathbf{G}}\mathbf{X} + \bar{\mathbf{C}}\mathbf{X} + \mathbf{F}(\mathbf{X}) = \mathbf{B}, \quad (2)$$

where  $\mathbf{X} \in \mathbb{R}^{N_h}$  is a vector of unknown cosine and sine coefficients for each of the variables in  $\mathbf{x}(t)$  and  $\mathbf{B} \in \mathbb{R}^{N_h}$  represents the contributions of the DC and AC independent sources. The size  $N_h$  of this system is typically very large due to the large number of harmonics and intermodulation products present in the case of multi tone inputs. Furthermore, the Jacobian of (2) is typically dense. This results in a large CPU cost in the computation of the system solution and the value of IP3.

## 4. Proposed method

In this paper, a new method for obtaining the IP3 is presented. Using the proposed approach the required Volterra kernels are computed numerically from the moments of (2). This approach does not require topology dependent analytical manipulations. It can therefore handle circuits with arbitrary complexity and nonlinearity. Furthermore it is to be noted that, IP3 is in fact obtained without the need to compute the solution of (2) which requires a large CPU cost due to the dense nature of the Jacobian and the number of Newton iterations required. Instead, the IP3 is computed from the system moments which only require one LU decomposition of a sparse matrix.

## 4.1. Calculation of the moments

The system moments are essentially the derivatives of the unknown solution vector  $\mathbf{X}$  with respect to the input voltage [2]. To develop the algorithm for calculating the moments efficiently, it is useful to express equation (2) in the following format

$$\bar{\mathbf{G}}\mathbf{X} + \bar{\mathbf{C}}\mathbf{X} + \mathbf{F}(\mathbf{X}) - \mathbf{B}_{dc} - \alpha\mathbf{B}_{ac} = 0 \quad (3)$$

In this expression,  $\alpha$  is the amplitude of the input signals and  $\mathbf{B}_{ac}$  is a vector with the only non-zero entries being entries of value '1' at the frequencies of interest.  $\mathbf{B}_{dc}$  is a vector containing the contributions of the DC independent sources. The system moments  $\mathbf{A}_0 \dots \mathbf{A}_q$  are then defined as the coefficients of the Taylor series of  $\mathbf{X}$  as a function of  $\alpha$  in

$$\begin{aligned} \mathbf{X} &= \mathbf{A}_0 + \mathbf{A}_1\alpha + \mathbf{A}_2\alpha^2 + \mathbf{A}_3\alpha^3 + \dots \\ &= \sum_{k=0}^q \mathbf{A}_k\alpha^k \end{aligned} \quad (4)$$

where  $\mathbf{A}_k$  is the  $k^{th}$  moment of the system. Once the moments are determined, the distortion analysis parameters can be obtained efficiently as will be shown in section 4.2.

For the purpose of analyzing distortion with little CPU cost, the moment vectors must be computed efficiently by the simulator. Next a method is presented to show how this task is performed. Substituting (4) into (3), we obtain the following:

$$\begin{aligned} \bar{\mathbf{G}} \sum_{k=0}^q \mathbf{A}_k\alpha^k + \bar{\mathbf{C}} \sum_{k=0}^q \mathbf{A}_k\alpha^k + \\ \sum_{k=0}^q \mathbf{D}_k\alpha^k - \mathbf{B}_{dc} - \alpha\mathbf{B}_{ac} = 0 \end{aligned} \quad (5)$$

where  $\mathbf{D}_k$  are the Taylor coefficients of  $\mathbf{F}(\mathbf{X})$  such that

$$\mathbf{F}(\mathbf{X}) = \sum_{k=0}^q \mathbf{D}_k\alpha^k \quad (6)$$

To solve for the zeroth moment  $\mathbf{A}_0$ , we set  $\alpha$  in (5) to zero. Setting  $\alpha = 0$ :

$$\bar{\mathbf{G}}\mathbf{A}_0 + \bar{\mathbf{C}}\mathbf{A}_0 + \mathbf{F}(\mathbf{A}_0) = \mathbf{B}_{dc} \quad (7)$$

Solving the above system to obtain  $\mathbf{A}_0$  is simply obtaining the DC solution of the system.

To solve for the remaining moments ( $\mathbf{A}_n$ ;  $n \geq 1$ ), we equate the powers of alpha in (5). Equating the first power of  $\alpha$ , we obtain

$$\bar{\mathbf{G}}\mathbf{A}_1 + \bar{\mathbf{C}}\mathbf{A}_1 + \mathbf{D}_1 = \mathbf{B}_{ac} \quad (8)$$

By applying the chain rule to  $\mathbf{D}_1 = \frac{\partial \mathbf{F}}{\partial \alpha}|_{\alpha=0} = \frac{\partial \mathbf{F}}{\partial \mathbf{X}} \cdot \frac{\partial \mathbf{X}}{\partial \alpha}|_{\alpha=0} = \mathbf{T}_0 \mathbf{A}_1$ , and substituting this expression into (8) we obtain

$$(\bar{\mathbf{G}} + \bar{\mathbf{C}} + \mathbf{T}_0) \mathbf{A}_1 = \mathbf{B}_{ac} \quad (9)$$

The first moment can now be obtained using one LU Decomposition to solve (9). It is important to note that the matrix  $(\bar{\mathbf{G}} + \bar{\mathbf{C}} + \mathbf{T}_0)$  is simply the sparse Jacobian matrix which is already computed when obtaining the DC solution. To obtain the remaining moments, we equate the  $n^{\text{th}}$  power of  $\alpha$  in (5) to obtain:

$$\bar{\mathbf{G}} \mathbf{A}_n + \bar{\mathbf{C}} \mathbf{A}_n + \mathbf{D}_n = 0 \quad n > 1 \quad (10)$$

To solve the system given in (10) efficiently for each value of  $n$ , we must express  $\mathbf{D}_n$  in a different manner. Using the chain rule we can express

$$\frac{\partial \mathbf{F}}{\partial \alpha} = \frac{\partial \mathbf{F}}{\partial \mathbf{X}} \cdot \frac{\partial \mathbf{X}}{\partial \alpha} = \mathbf{T} \frac{\partial \mathbf{X}}{\partial \alpha}, \quad (11)$$

where

$$\mathbf{T}(\alpha) = \frac{\partial \mathbf{F}(\mathbf{X})}{\partial \mathbf{X}} = \sum_{k=0} \mathbf{T}_k \alpha^k \quad (12)$$

Substituting (4), (6) and (12) into (11) we obtain

$$\sum_{i=1}^q i \mathbf{D}_i \alpha^{i-1} = \sum_{i=0}^q \mathbf{T}_i \alpha^i \sum_{i=1}^q i \mathbf{A}_i \alpha^{i-1} \quad (13)$$

To solve for  $\mathbf{D}_n$ , we take the  $n^{\text{th}}$  derivative of (13) and set  $\alpha$  to zero. We can then express  $\mathbf{D}_n$  as

$$\mathbf{D}_n = \mathbf{T}_0 \mathbf{A}_n + \frac{1}{n} \sum_{j=1}^{n-1} (n-j) \mathbf{T}_j \mathbf{A}_{n-j} \quad (14)$$

Substituting (14) into (10) and rearranging yields

$$(\bar{\mathbf{G}} + \bar{\mathbf{C}} + \mathbf{T}_0) \mathbf{A}_n = -\frac{1}{n} \sum_{j=1}^{n-1} (n-j) \mathbf{T}_j \mathbf{A}_{n-j} \quad (15)$$

This recursive relationship is used to calculate the remaining moments. The right-hand side of equation (15) is calculated using the values of the previous moments ( $\mathbf{A}_{n-j}$ ) that have already been obtained, in addition to the values of the partial derivatives of the non-linear vector functions with respect to the solution vector ( $\mathbf{T}_j$ ). All that remains is to show how to obtain these terms. Since  $\mathbf{F}(\mathbf{X})$  and  $\mathbf{X}$  are vectors, the term  $\mathbf{T}(\alpha)$  in (12) will be a matrix of the form

$$\mathbf{T}(\alpha) = \frac{\partial \mathbf{F}(\mathbf{X})}{\partial \mathbf{X}} = \begin{bmatrix} \frac{\partial F_1}{\partial X_1} & \cdots & \frac{\partial F_1}{\partial X_n} \\ \vdots & \ddots & \vdots \\ \frac{\partial F_n}{\partial X_1} & \cdots & \frac{\partial F_n}{\partial X_n} \end{bmatrix} \quad (16)$$

where each  $\frac{\partial F_i}{\partial X_i}$  term is a block matrix in itself. To simplify the presentation of calculating these terms, we will only consider one of the terms in the  $\mathbf{T}(\alpha)$  matrix shown in (16),  $\frac{\partial F_1}{\partial X_1}$ . If we represent  $\frac{\partial F_1}{\partial X_1}$  as matrix  $\mathbf{T}_{11}$  and express it as a Taylor series expansion we then have

$$\frac{\partial F_1}{\partial X_1} = \mathbf{T}_{11} = \mathbf{P} = \sum_{j=0} \mathbf{P}_j \alpha^j \quad (17)$$

where the Taylor coefficient  $\mathbf{P}_j$  is entered in  $\mathbf{T}_j$  at the location corresponding to  $\frac{\partial F_1}{\partial X_1}$ . The  $\mathbf{P}_j$  matrices are computed using

$$\mathbf{P}_j = \mathbf{\Gamma}^{-1} \begin{bmatrix} \frac{\partial f_1(x_1(t_1))}{\partial x_1} & & 0 \\ & \ddots & \\ 0 & & \frac{\partial f_1(x_1(t_s))}{\partial x_1} \end{bmatrix} \mathbf{\Gamma} \quad (18)$$

where  $t_1$  to  $t_s$  are the time sample points equally spaced over the fundamental period (note that frequency mapping and diamond truncation [5] is used in order to handle quasi-periodic inputs efficiently using FFT), and  $\mathbf{\Gamma}$  is the Inverse DFT matrix defined as

$$\mathbf{\Gamma} = \begin{bmatrix} 1 & \cos(\Theta_{0,1}) & \sin(\Theta_{0,1}) & \cdots & \cos(\Theta_{0,H}) & \sin(\Theta_{0,H}) \\ \vdots & \vdots & \vdots & \ddots & \vdots & \vdots \\ 1 & \cos(\Theta_{n,1}) & \sin(\Theta_{n,1}) & \cdots & \cos(\Theta_{n,H}) & \sin(\Theta_{n,H}) \\ \vdots & \vdots & \vdots & \ddots & \vdots & \vdots \\ 1 & \cos(\Theta_{N_i,1}) & \sin(\Theta_{N_i,1}) & \cdots & \cos(\Theta_{N_i,H}) & \sin(\Theta_{N_i,H}) \end{bmatrix} \quad (19)$$

with

$$\Theta_{n,k} = kn \left( \frac{2\pi}{N_h} \right) \quad (20)$$

and  $N_i = N_h - 1$ . Note that the matrix-vector multiplication with  $\mathbf{\Gamma}$  and  $\mathbf{\Gamma}^{-1}$  can be done efficiently by taking advantage of the Fast Fourier Transform (FFT), and Inverse Fast Fourier Transform (IFFT) algorithms. It is also to be noted that the Jacobian is the same for all moments as can be seen from (9) and (15). Furthermore, since the expansion is at the DC operating point ( $\mathbf{A}_0$  is the DC solution), this Jacobian is very sparse.

## 4.2. Computation of IP3

In order to simplify the presentation, we first consider a memoryless system. The output variable  $y$  is expressed as a power series of the input  $v$ . The input output relationship can be written as,

$$y = k_0 + k_1 v + k_2 v^2 + k_3 v^3 + \cdots = \sum_n k_n v^n \quad (21)$$

Substituting  $v = \alpha(\cos(\omega_1 t) + \cos(\omega_2 t))$  into (21), truncating after  $k_3$ , and expanding using trigonometric identities we obtain

$$\begin{aligned}
y = & k_0 + (k_1 \cos(\omega_1 t) + k_1 \cos(\omega_2 t))\alpha \\
& + (k_2 + \frac{k_2}{2} \cos(2\omega_1 t) + k_2 \cos((\omega_1 + \omega_2)t) \\
& + k_2 \cos((\omega_1 - \omega_2)t) + \frac{k_2}{2} \cos(2\omega_2 t))\alpha^2 \\
& + (\frac{9k_3}{4} \cos(\omega_1 t) + \frac{k_3}{4} \cos(3\omega_2 t) \\
& + \frac{9k_3}{4} \cos(\omega_2 t) + \frac{k_3}{4} \cos(3\omega_1 t) \\
& + \frac{3k_3}{4} \cos((2\omega_2 - \omega_1)t) + \frac{3k_3}{4} \cos((2\omega_1 + \omega_2)t) \\
& + \frac{3k_3}{4} \cos((2\omega_2 + \omega_1)t) + \frac{3k_3}{4} \cos((2\omega_1 - \omega_2)t))\alpha^3
\end{aligned} \tag{22}$$

By comparing (22) with (4), the relationship between  $k_n$  and the system moments can be deduced as shown in Table 1 [10].

In the presence of memory elements such as capacitors and inductors, similarly to the memoryless case shown in Table 1 which shows the relation between the Taylor coefficients and the circuit moments, an equivalent table for memory systems can be derived which relates the system moments to the Volterra kernels [11]. For example,  $|H_1(j\omega_1)|$  is related to the entry corresponding to the frequency  $\omega_1$  in the moment  $\mathbf{A}_1$ , and  $|H_3(j\omega_1, j\omega_1, -j\omega_2)|$  is related to the entry corresponding to  $2\omega_1 - \omega_2$  in the moment vector  $\mathbf{A}_3$ . The third order intercept point (IP3) can then be found by using the following relation [11]

$$IIP_3 = \frac{2}{\sqrt{3}} \sqrt{\frac{|H_1(j\omega_1)|}{|H_3(j\omega_1, j\omega_1, -j\omega_2)|}} \tag{23}$$

The above relation is for the Low Side IIP3. To obtain the High Side IIP3 we replace  $|H_1(j\omega_1)|$  by  $|H_1(j\omega_2)|$  and  $|H_3(j\omega_1, j\omega_1, -j\omega_2)|$  by  $|H_3(j\omega_1, -j\omega_2, -j\omega_2)|$  [11]. For the case of circuits with memoryless elements, the value of IIP3 will be the same regardless of whether the low side or high side intermodulation term was considered. Once IIP3 is obtained using (23), the value of OIP3 can be computed by multiplying the result by  $|H_1(j\omega_1)|$ .

It is important to note that the Jacobian matrix used in this proposed method is constant and is at the DC operating point. Therefore it is very sparse unlike a typical Harmonic Balance Jacobian matrix, and only one LU decomposition is required throughout the solution process. In contrast, the brute force simulation based approach requires the solution of a system of equations with a dense Jacobian at each Newton iteration which requires high CPU cost. It is also important to note that other terms used for analyzing distortion,

**Table 1. Location of Taylor series coefficients in moment vectors.**

Frequency	$\mathbf{A}_0$	$\mathbf{A}_1$	$\mathbf{A}_2$	$\mathbf{A}_3$
DC	$k_0$	0	$k_2$	0
$2\omega_1 \pm \omega_2$	0	0	0	$\frac{3}{4}\mathbf{k}_3$
$\omega_1$	0	$\mathbf{k}_1$	0	$\frac{9}{4}k_3$
$\omega_2$	0	$\mathbf{k}_1$	0	$\frac{9}{4}k_3$
$2\omega_2 \pm \omega_1$	0	0	0	$\frac{3}{4}\mathbf{k}_3$
$2\omega_1$	0	0	$\frac{1}{2}k_2$	0
$2\omega_2$	0	0	$\frac{1}{2}k_2$	0

such as the Second Order Intercept Point (*IP2*) and Harmonic Distortion (*HD*), can be computed by extracting the appropriate Volterra kernels from the moments.

## 5. Examples

In this section, numerical results of simulations performed on two example circuits are shown in order to illustrate the proposed approach. The value of IP3 obtained using the proposed method, which does not require a harmonic balance solution, is compared with that obtained using the brute force method which is based on multi-tone harmonic balance simulation. As was expected the results were identical.

### 5.1. Example 1

The first example considered is a common emitter Low Noise Amplifier (LNA) with an LC tank centered at 1GHz, and input and output matching networks as shown in Fig. 1. In order to measure the linearity of the circuit the brute force method was first used by applying two -50 dBm input tones,  $f_1 = 1$  GHz and  $f_2 = 1.01$  GHz, and performing a standard harmonic balance analysis. The results are shown in Fig. 2 and Fig. 3. The calculated IIP3 in this case was -12.02 dBm and the Output IP3 (OIP3) was found to be -7.79 dBm. This simulation was run with 10 harmonics, therefore the size of the dense Jacobian which had to be solved was  $3315 \times 3315$  due to 10 harmonics of the fundamental tones in addition to the intermodulation tones truncated using diamond truncation [5].

The distortion was then analyzed using the proposed approach by computing the moments of the system and extracting the Volterra kernels at the appropriate frequencies.

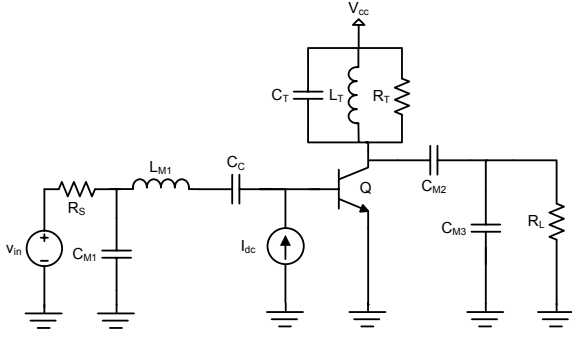


Figure 1. Circuit diagram of example 1.

The resulting values of IIP3 and OIP3 were found to be -12.02 dBm and -7.79dBm respectively. As can be seen, the results are consistent with the brute force approach based on Harmonic Balance simulations. The error between the two methods was less than 0.01%.

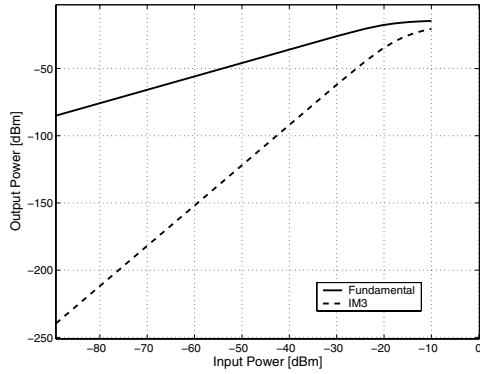


Figure 2. Output power of fundamental and IM3 tones of example 1.

## 5.2. Example 2

The second example considered is the differential cascode LNA circuit shown in Fig. 4. This amplifier is biased using a DC Current Source in the emitter and also with DC voltage biasing at the bases of the transistors. The biasing circuitry is not shown in the diagram and neither are the matching networks to  $50\Omega$  source and load impedances. The current source is implemented using a current mirror topology. This amplifier has a differential voltage gain of 18.3dB. Linearity was measured first using the brute force approach by applying two -70dBm input tones,  $f_1 = 1$  GHz and  $f_2 = 1.01$  GHz, and performing a standard harmonic balance analysis. The results are shown in Fig. 5 and Fig. 6. The measured IIP3 in this case was found to be -13.89 dBm, and the OIP3 was 4.63 dBm. This simulation was

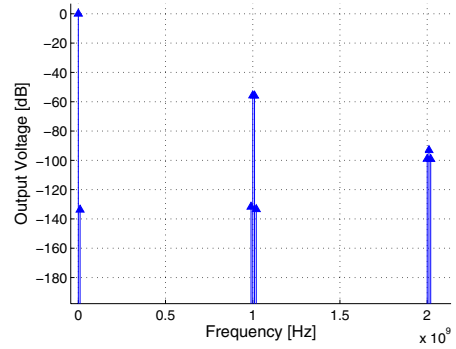


Figure 3. Output voltage spectrum for circuit of example 1.

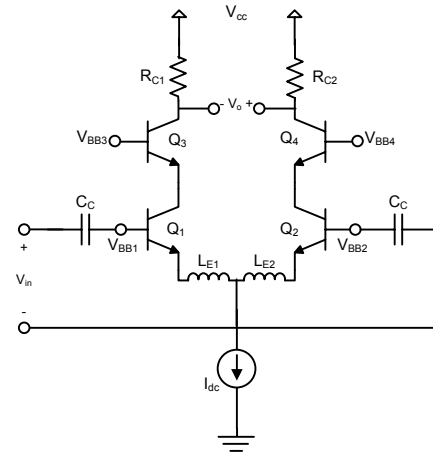


Figure 4. Circuit diagram of example 2.

run with 10 harmonics, therefore the size of the dense Jacobian which had to be solved was  $9061 \times 9061$  due to 10 harmonics of the fundamental tones in addition to the diamond truncation tones.

The distortion was then analyzed using the proposed approach by computing the moments of the system and extracting the Volterra kernels at the appropriate frequencies. The resulting values of IIP3 and OIP3 were found to be -13.87 dBm and -4.63 dBm respectively. The results are consistent with the brute force approach and the error between the two approaches was less than 0.02%.

## 5.3. CPU cost comparison

The data in Table 2 shows a comparison of the CPU times and the speed-up between the proposed method and the HB solution using a prototype Matlab simulator. The speed-up over a harmonic balance simulation was 19.8 times for Example 1, and 64.6 times for Example 2. This

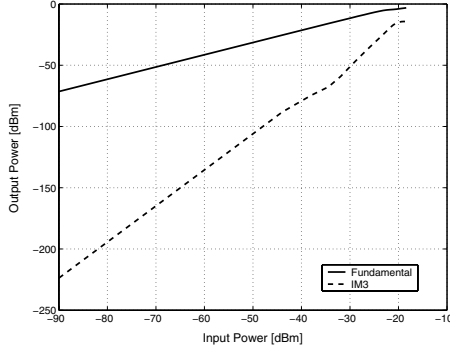


**Figure 5. Output power of fundamental and IM3 tones of example 2.**

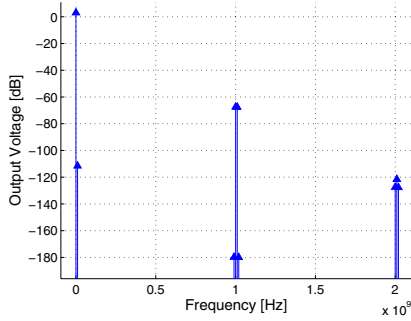


**Figure 6. Output voltage spectrum for example 2.**

speed-up is due to three main reasons. Firstly, the moments used in the proposed method are found by solving a linear equation without the need for any Newton Iteration. Secondly, the left-hand-side matrix in (15) for finding the moments is the same for all moments, while the Harmonic Balance Jacobian is different at each Newton Iteration. Finally the HB Jacobian is significantly more dense than the Jacobian used for solving for the moments. For Example 2, the  $9061 \times 9061$  HB Jacobian contains 2,033,113 non-zero elements while the  $9061 \times 9061$  matrix for finding the moments contains only 36,875 non-zeros. As a result, the CPU time needed for 1 LU decomposition of the HB Jacobian was 1.14 seconds for Example 1 and 19.98 seconds for Example 2 as opposed to 0.016 seconds and 0.078 seconds, respectively, for 1 LU decomposition of the matrix for finding the moments. It is also important to note that the greater the number of non-linear elements present in the system, the more significant is the speed-up between the two approaches as can be seen when comparing the results of Example 1 to those of Example 2.

**Table 2. Comparison of CPU times between the proposed method and the HB solution.**

	HB Solution	Proposed Method	Speed-up
Ex. 1	11.14 s	0.562 s	19.8
Ex. 2	197.80 s	3.063 s	64.6

## 6. Conclusion

In this paper, a new simulation method for measuring distortion at the output of a non-linear system based on the calculation of the system moments was presented. The new approach is applicable to arbitrary circuit topologies and was shown to be as accurate as brute force techniques based on Harmonic Balance simulation, while providing significant CPU speed-up.

## References

- [1] R. Baki, C. Beainy, and M. N. El-Gamal. Distortion analysis of high frequency log-domain filters using volterra series. *Circuits and Systems II: Analog and Digital Signal Processing*, 50, 2003.
- [2] R. Griffith and M. Nakhla. A new high order absolutely stable explicit numerical integration algorithm for the time domain simulation of nonlinear circuits. In *Proc. ACM IC-CAD*, pages 504–509, 1997.
- [3] C. W. Ho, A. E. Ruehli, and P. A. Brennan. The modified nodal approach to network analysis. *IEEE Trans. Circuits Syst.*, 22(6):504–509, June 1975.
- [4] K. Kundert and A. Sangiovanni-Vincentelli. Simulation of nonlinear circuits in the frequency domain. *IEEE Trans. Computer-Aided Design*, 5(4):521–535, Oct. 1986.
- [5] K. S. Kundert, J. K. White, and A. Sangiovanni-Vincentelli. *Steady-State Methods for Simulating Analog and Microwave Circuits*. Kluwer Academic, Boston, 1990.
- [6] S. Maas. *Nonlinear Microwave and RF Circuits*. Artech House Publishers, Upper Saddle River, NJ, 2003.
- [7] M. S. Nakhla and J. Vlach. A piecewise harmonic-balance technique for determination of periodic response of nonlinear systems. *IEEE Trans. Circuits Syst.*, 23(2):85–91, Feb. 1976.
- [8] B. Razavi. *RF Microelectronics*. Prentice-Hall, New Jersey, 1998.
- [9] W. Reiss. Nonlinear distortion analysis of p-i-n diode attenuators using volterra series representation. *Circuits and Systems*, 1984.
- [10] J. Rogers and C. Plett. *Radio Frequency Integrated Circuit Design*. Artech House, Inc., Norwood, MA, 2003.
- [11] P. Wambacq and W. Sansen. *Distortion Analysis of Analog Integrated Circuits*. Kluwer Academic Publishers, The Netherlands, 1998.